Salidroside Prevents Hypoxia-Induced Human Retinal Microvascular Endothelial Cell Damage Via miR-138/ROBO4 Axis

Xiaoling Shi,[1,2] Nuo Dong,[2] Qi Qiu,[1] Shanhua Li,[1] and Jiaxing Zhang[1]

[1]Institute of Brain Diseases and Cognition, Medical College of Xiamen University, Xiamen, Fujian, China
[2]Affiliated Xiamen Eye Center, Medical College of Xiamen University, Xiamen, Fujian, China

PURPOSE. Retinopathies are associated with the injury of retinal microvascular endothelial cells. Salidroside (SAL) is a medicinal supplement that has antioxidative and cytoprotective properties. We hypothesized that SAL might have a protective function in retinopathies. This research aims to explore the function and mechanism of SAL in hypoxia-induced retinal microvascular endothelial cell injury.

METHODS. Human retinal microvascular endothelial cells (HRMECs) injury was induced by culturing under hypoxic condition. The function of SAL on HRMECs injury was investigated using cell counting kit-8, 5-ethynyl-2′-deoxyuridine (EdU) staining, flow cytometry, Western blotting, and enzyme linked immunosorbent assay. MicroRNA (miR)-138, roundabout 4 (ROBO4), and proteins in the phosphoinositide 3-kinase (PI3K)/protein kinase B (AKT)/mammalian target of rapamycin (mTOR) pathways were examined using quantitative reverse transcription polymerase chain reaction or Western blotting. The target correlation was determined by dual-luciferase reporter analysis and RNA immunoprecipitation.

RESULTS. Hypoxia resulted in proliferation inhibition, cycle arrest, apoptosis, inflammatory reaction, and oxidative stress in HRMECs. SAL attenuated hypoxia-induced HRMECs injury via increasing cell proliferation, and mitigating cycle arrest, apoptosis, inflammatory reaction, and oxidative stress. MiR-138 expression was enhanced by hypoxia, and decreased via SAL stimulation. MiR-138 upregulation reversed the influence of SAL on hypoxia-induced HRMECs injury. ROBO4 was targeted via miR-138. ROBO4 overexpression weakened the role of miR-138 in HRMECs injury. The PI3K/AKT/mTOR pathway was inactivated under hypoxic condition, and SAL increased the activation of PI3K/AKT/mTOR pathways by decreasing miR-138.

CONCLUSIONS. SAL protected against hypoxia-induced HRMECs injury through regulating miR-138/ROBO4 axis, indicating the protective potential of SAL in retinopathies.

Keywords: retinal microvascular endothelial cell, salidroside, hypoxia, miR-138, ROBO4

The ischemic retinopathies are related to endothelial dysfunction that is associated with retinal neovascularization, which is the main cause of vision loss.[1] Hypoxia inhibits vascular development in ischemic retinopathies.[2] Moreover, hypoxia can induce retinal microvascular endothelial cell dysfunction, which contributes to the development of ischemic retinopathies.[3,4] Thus, exploring new strategies for attenuating hypoxia-induced retinal microvascular endothelial cell damage might be of importance for the treatment of ischemic retinopathies.

Salidroside (SAL) is a medicinal supplement mostly in the roots of *Rhodiola spp*, which has diverse biological properties, like anti-inflammation, anti-apoptosis, anti-oxidation, etc.[5–8] Moreover, SAL can prevent hypoxia-induced injury in neural stem cells or liver dysfunction.[9,10] Additionally, SAL protects against hydroperoxide or high-glucose-induced retinal pigment epithelial damage.[11,12] Here, we hypothesized SAL might play a protective role in retinal microvascular endothelial cells under hypoxia condition. However, the

pharmacological activity of SAL in hypoxia-induced retinal microvascular endothelial cell damage remains unclear.

MicroRNAs (miRNAs) are short noncoding RNAs that participate in translational repression and mRNA degeneration, which are associated with retinal neovascularization and retinal endothelial cell dysfunction.[13,14] Moreover, miRNAs are the response to SAL stimulation.[9,12] MiR-138 is an important miRNA associated with hypoxia-induced endothelial dysfunction.[15] In addition, SAL can induce miR-138 downregulation, thus to attenuate high-glucose-induced injury of retinal pigment epithelial cells.[12] However, it is unknown whether SAL can target miR-138 to regulate hypoxia-induced retinal microvascular endothelial cell damage. Roundabout 4 (ROBO4) is an endothelial-specific transmembrane receptor that regulates vascular permeability and neovascularization.[16] Furthermore, upregulated ROBO4 is induced by hyperglycemia, and it contributes to retinal microvascular endothelial cell dysfunction.[17] Although ROBO4 expression is decreased in

retinal microvascular endothelial cells under hypoxic condition, indicating that ROBO4 might have different roles in various types of cell injury.[18] Yet, no study reports the function of ROBO4 in hypoxia-induced retinal microvascular endothelial cell damage.

We hypothesized SAL might regulate retinal microvascular endothelial cell damage under hypoxia condition through the miR-138/ROBO4 axis. In this study, retinal microvascular endothelial cells were treated with hypoxia stimulation. The purposes of this research were to study the pharmacological function of SAL in hypoxia-induced retinal microvascular endothelial cell damage, and to explore whether it was associated with an miR-138/ROBO4 axis.

MATERIALS AND METHODS

Cell Culture and Treatment

Human retinal microvascular endothelial cells (HRMECs; cat. no. CP-H130) were provided by Procell (Wuhan, China), and grown in the specific complete culture medium for HRMECs (cat. no. CM-H130; Procell) containing 10% fetal bovine serum, growth supplement, and 1% antibiotic under $37°C$ in 5% CO_2.

Experimental Design and Cell Treatment

To induce hypoxic injury, HRMECs were cultured under 1% O_2 for 24 hours, and cells under normoxic condition were set as the control group. To explore the function of SAL, HRMECs were pretreated with 5, 10, or 20 µg/mL SAL (MedChemExpress, Monmouth Junction, NJ, USA) for 24 hours before hypoxia stimulation. The cells in corresponding nontreated group were exposed to equal volume of DMSO prior to hypoxia stimulation. To explore the effect of miR-138 and ROBO4, corresponding cell transfection was performed before treatment with SAL and hypoxia stimulation.

Cell Transfection

The pcDNA3.1-based ROBO4 overexpression vector (pc-ROBO4) was generated via inserting the sequence of ROBO4 in the vector, and the empty vector (Thermo Fisher Scientific, Waltham, MA, USA) was utilized as negative control (pc-NC). MiR-138 mimic (5′-AGCUGGUGUUGUGAAUCAGGCCG-3′), and mimic negative control (miRNA NC; 5′-CGAUCGCAUCAGCAUCGAUUGC-3′) were provided via iGeneBio (Guangzhou, China). HRMECs were transfected with 800 ng vectors or 30 nM mimics using Lipofectamine 3000 (Thermo Fisher Scientific) for 24 hours.

Quantitative Reverse Transcription Polymerase Chain Reaction

HRMECs were lysed in Trizol (Thermo Fisher Scientific) for RNA extraction. The reverse transcription was processed using 800 ng RNA and a miRNA reverse transcription kit (Thermo Fisher Scientific). The generated cDNA was mixed with SYBR Green (Vazyme, Nanjing, China) and primer pairs (Sangon, Shanghai, Chian), and used for quantitative reverse transcription polymerase chain reaction (qRT-PCR). The specific primer pairs were displayed as follows: miR-138 (sense: 5′-GCCGAGAGCTGGTGTTGTGAA-3′; antisense: 5′-CAGTGCGTGTCGTGGAGT-3′), and

U6 (sense, 5′-CTCGCTTCGGCAGCACA-3′; antisense, 5′-AACGCTTCACGAATTTGCGT-3′). Relative expression of miR-138 was calculated with U6 as a reference according to the $2^{-\Delta\Delta Ct}$ method.[19]

Cell Counting kit-8

HRMECs (1×10^4/well) were dispersed in 96-well plates, and subjected to hypoxia stimulation for 24 hours. Then 10 µL cell counting kit-8 (CCK-8; Beyotime, Shanghai, China) was added, and cells were incubated for 4 hours. The absorbance at 450 nm was examined through a microplate reader (Bio-Rad, Hercules, CA, USA). Cell viability was calculated by normalizing to the control group × 100%.

5-Ethynyl-2′-Deoxyuridine (EdU) Staining

HRMECs (2×10^5/well) were dispersed in 6-well plates, and incubated under hypoxic condition for 24 h. Then cell proliferation was analyzed utilizing a 5-ethynyl-2′-deoxyuridine (EdU) staining cell proliferation assay kit (Merck Millipore, Billerica, MA, USA) according to the manufacturer's instruction. The nuclei were labeled with 4′,6-diamidino-2-phenylindole (DAPI; Solarbio, Beijing, China). The EdU-positive cells were observed through a fluorescence microscope (Olympus, Tokyo, Japan).

Flow Cytometry

Flow cytometry was utilized to detect cycle distribution and apoptosis. For cycle process analysis, 1×10^5 HRMECs were added in 12-well plates, and cultured under hypoxic condition for 24 hours, followed by fixture with 70% ethanol (Aladdin, Shanghai, China). After dyeing to 5 µL propidium iodide (PI; Solarbio) for 10 minutes, cycle distribution was examined through a flow cytometer (BD Biosciences, San Jose, CA, USA).

For apoptosis analysis, Annexin V-fluorescein isothiocyanate (FITC) apoptosis detection kit (Beyotime) was used. Briefly, 2×10^5 HRMECs were dispersed in 12-well plates, and incubated under hypoxic condition for 24 hours. Then, cells were collected and resuspended in Annexin V binding buffer. After staining with Annexin V-FITC and PI for 10 minutes, apoptotic cells were examined with a flow cytometer.

Western Blotting

HRMECs were lysed in radio-immunoprecipitation assay buffer (Thermo Fisher Scientific) with 1% protease and phosphatase inhibitors (Thermo Fisher Scientific) for protein isolation, and protein concentration was determined using a bicinchoninic acid assay kit (Thermo Fisher Scientific). Protein samples (20 µg) were separated via sodium dodecyl sulfate-polyacrylamide gel electrophoresis, and transferred on polyvinylidene fluoride membranes (Merck Millipore). The membranes were blocked in 3% bovine serum albumin (Solarbio), and then incubated with primary antibodies overnight and secondary antibody for 2 hours. The antibodies (Abcam, Cambridge, UK) included: anti-proliferating cell nuclear antigen (PCNA; ab92552, 1:5000 dilution), anti-cyclin D1 (ab226977, 1:3000 dilution), anti-Bcl-2 related X protein (Bax; ab104156, 1:500 dilution), anti-B-cell lymphoma-2 (Bcl-2; ab196495, 1:2000 dilution), anti-ROBO4 (ab272734, 1:1000 dilution), anti-phosphoinoside 3-kinase

(PI3K; ab133595, 1:1000 dilution), anti-phosphorylated (p)-PI3K (ab182651, 1:500 dilution), anti-protein kinase B (AKT; ab18785, 1:1000 dilution), anti-p-AKT (ab38449, 1:500 dilution), anti-mammalian target of rapamycin (mTOR; ab32028, 1:2000 dilution), anti-p-mTOR (ab109268, 1:1000 dilution), anti-β-actin (ab8227, 1:5000 dilution), and IgG labeled via horseradish peroxidase (ab205718, 1:10000 dilution). The blots were visualized using BeyoECL Plus kit (Beyotime), and then analyzed with β-actin as reference by Quantity One software (Bio-Rad).

Enzyme Linked Immunosorbent Assay

HRMECs (5×10^4/well) were dispersed in 24-well plates, and incubated under hypoxic condition for 24 hours. Next, culture supernatants were collected, and used for detecting tumor necrosis factor alpha (TNF-α), interleukin (IL)-6 and IL-8 levels using TNF-α, IL-6, or IL-8 ELISA kits (Thermo Fisher Scientific) according to the manufacturer's instruction. The absorbance was determined through a microplate reader at 450 nm. The secretion levels of TNF-α, IL-6, or IL-8 were calculated according to the standard curve, and normalized to the protein concentration and the control group.

Malondialdehyde, Reactive Oxygen Species, and Superoxide Dismutase Assays

A cellular reactive oxygen species (ROS) assay kit (Abcam) was used to detect ROS level. In brief, 2×10^4

HRMECs were dispersed in 96-well plates, and subjected to hypoxia stimulation for 24 hours. Next, cells were incubated with 10 μM DCFH-DA for 30 minutes, and then detected by a fluorescence microplate (Molecular Devices, Sunnyvale, CA, USA) at Ex/Em = 490/525 nm. Relative ROS level was normalized to the control group.

For malondialdehyde (MDA) and superoxide dismutase (SOD) assays, 2×10^4 HRMECs were placed in 96-well plates, and incubated under hypoxic condition for 24 hours. Then, culture supernatants were collected, and MDA and SOD levels were detected using MDA or SOD assay kit (Sigma-Aldrich, St. Louis, MO, USA) according to the manufacturer's instruction. The absorbance was measured with a microplate reader at 532 nm for MDA or 450 nm for SOD. Relative MDA and SOD levels were expressed as fold change of the control group.

Dual-Luciferase Reporter and RNA Immunoprecipitation Assays

The binding sites between miR-138 and ROBO4 were predicted by starBase.[20] The wild-type (WT) or mutant (MUT) sequence of ROBO4 3′UTR with miR-138 target sites was cloned into pGL3-Basic vector (Promega, Madison, WI, USA), generating the WT-ROBO4-3′UTR and MUT-ROBO4-3′UTR luciferase reporter vectors. The WT-ROBO4-3′UTR or MUT-ROBO4-3′UTR vector was co-transfected with miRNA NC or miR-138 mimic in HRMECs.
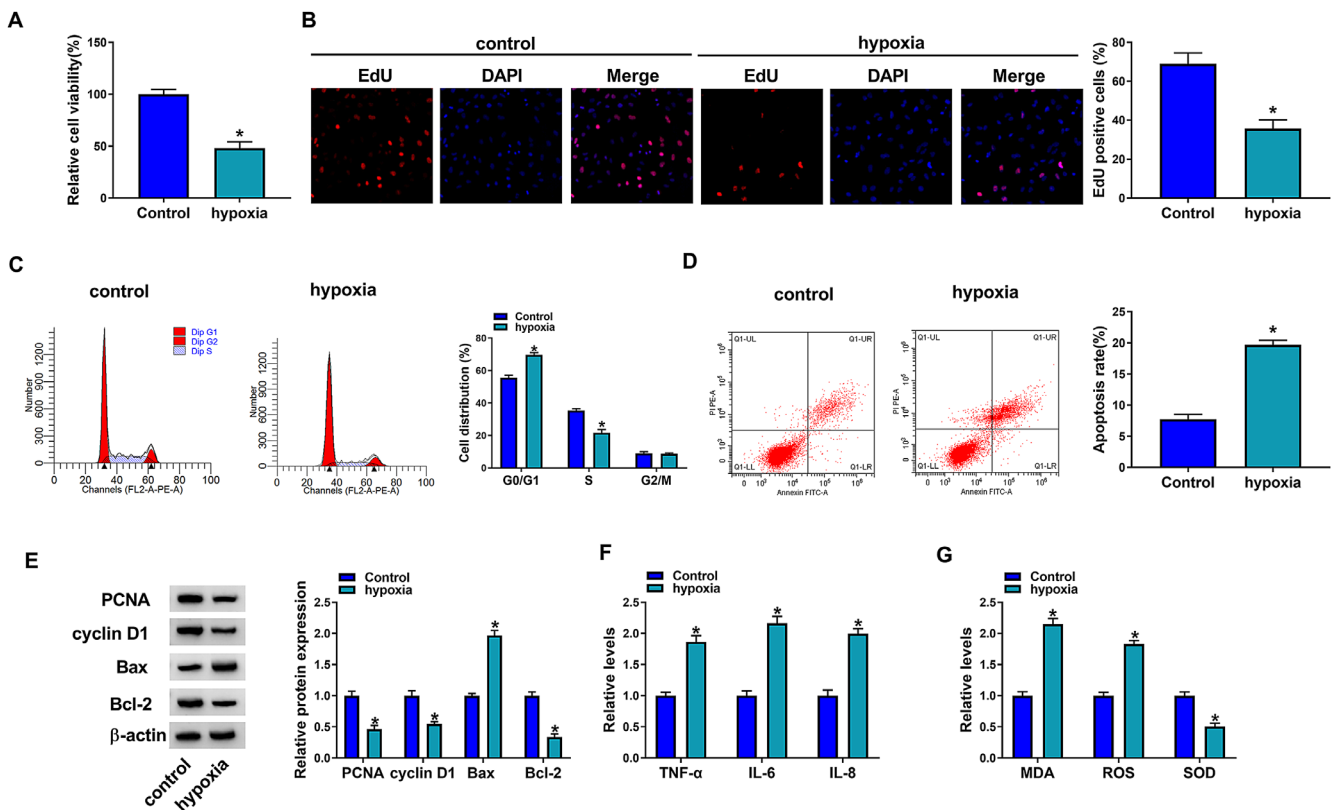
FIGURE 1. HRMECs injury under hypoxic condition. HRMECs were cultured under hypoxic or control (normoxic) condition for 24 hours. Cell viability (**A**), proliferation (**B**), cycle process (**C**), apoptosis (**D**), protein levels of PCNA, cyclinD1, Bax, and Bcl-2 (**E**), secretion levels of TNF-α, IL-6, and IL-8 (**F**), and levels of MDA, ROS, and SOD (**G**) were detected using CCK-8, EdU staining, flow cytometry, Western blotting, and ELISA. *$P < 0.05$.

The luciferase activity was examined using a dual-luciferase assay kit (Promega) after 24 hours of post-transfection.

RNA Immunoprecipitation (RIP) assay was processed with a Magna RIP kit (Merck Millipore). In brief, 1×10^7 HRMECs were lysed using RIP lysis buffer, and then incubated with Ago2-coated magnetic beads overnight. IgG was used as negative control. Enriched miR-138 and ROBO4 levels were detected.

Statistical Analysis

Data were displayed as mean ± standard deviation (SD) from three independent experiments with four technical replicates. Statistical analysis was processed through GraphPad Prism 8 (GraphPad, La Jolla, CA, USA). The difference was compared using Student's *t*-test or 1-way ANOVA followed by Tukey post hoc test. It was significant when $P < 0.05$.

RESULTS

Hypoxia Induces HRMECs Injury

The retinal microvascular endothelial cell injury model was established by culturing HRMECs under hypoxic condition for 24 hours. After hypoxia stimulation, HRMECs viability was significantly decreased (Fig. 1A)). Furthermore, hypoxia stimulation clearly decreased HRMECs proliferation by reducing EdU-positive cell number (Fig. 1B). In addition, hypoxia treatment led to cell cycle arrest at G0/G1 phase and higher apoptosis in HRMECs (Figs. 1C, 1D). Moreover, related proteins were detected in HRMECs. Results showed PCNA, cyclin D1, and Bcl-2 levels were markedly decreased, but Bax expression was enhanced after hypoxia treatment (Fig. 1E). Additionally, pro-inflammatory cytokines (TNF-α, IL-6, and IL-8) levels were markedly elevated in HRMECs after hypoxia treatment (Fig. 1F). Besides, hypoxia challenge obviously promoted MDA and ROS levels, while inhibited SOD level in HRMECs (Fig. 1G). These results
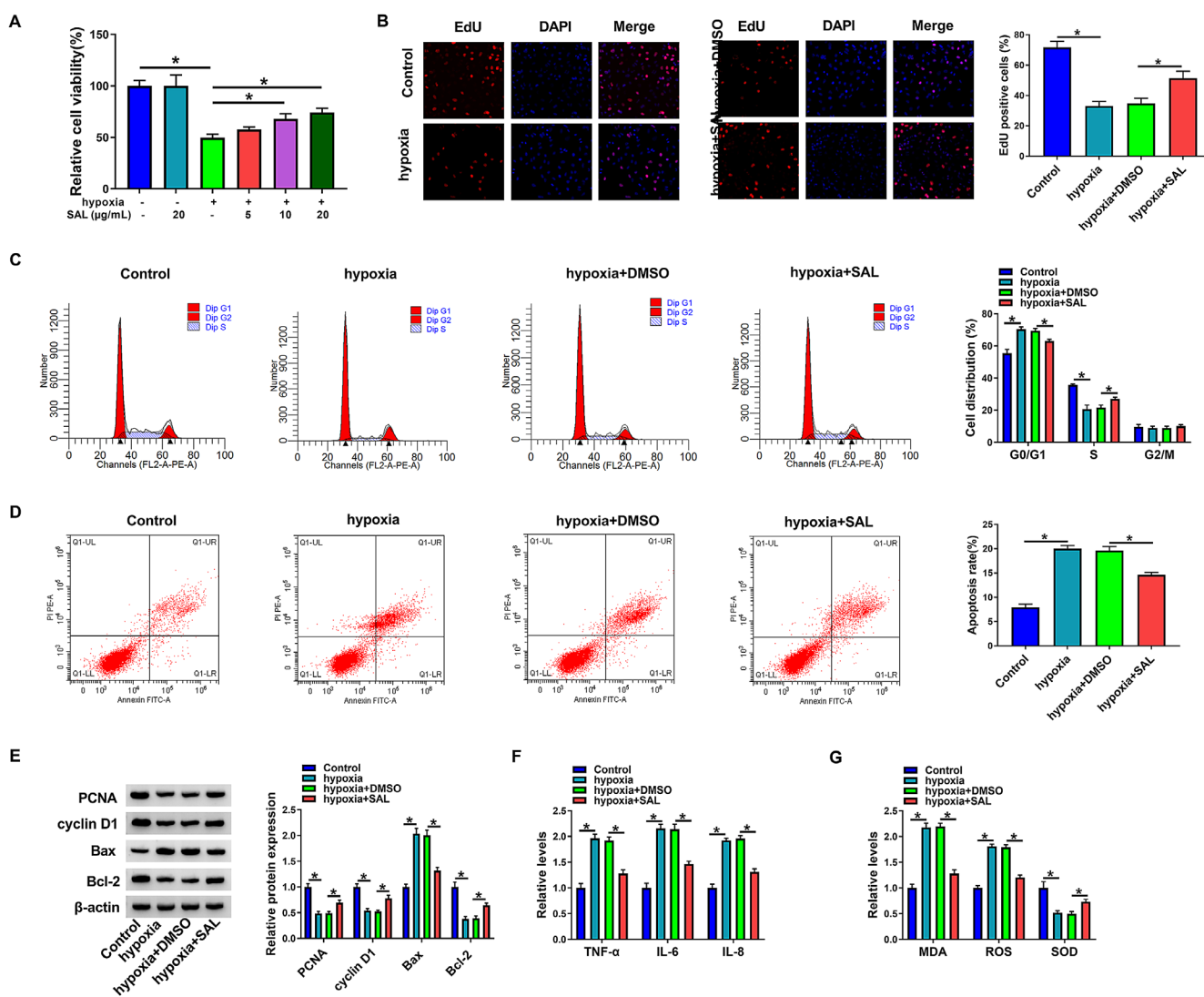
FIGURE 2. **Effect of SAL on HRMECs injury under hypoxic condition.** (**A**) HRMECs viability was measured by CCK-8 after stimulation with hypoxia or SAL for 24 hours. HRMECs were stimulated with 20 μg/mL SAL for 24 hours before hypoxic treatment for 24 hours. Cell proliferation (**B**), cycle process (**C**), apoptosis (**D**), protein levels of PCNA, cyclinD1, Bax, and Bcl-2 (**E**), secretion levels of TNF-α, IL-6, and IL-8 (**F**), and levels of MDA, ROS, and SOD (**G**) were examined using EdU staining, flow cytometry, Western blotting, and ELISA. *$P < 0.05$.
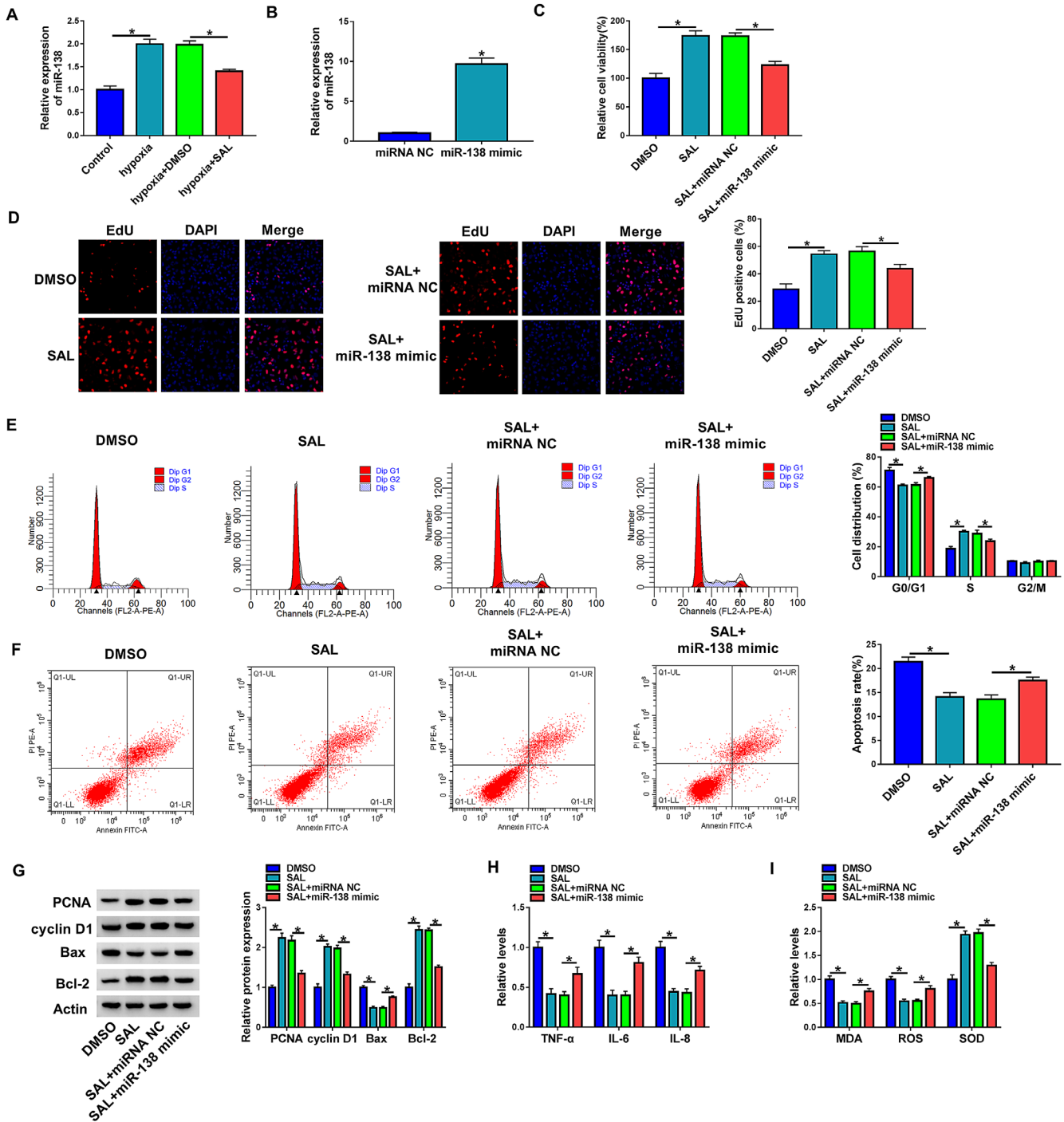
FIGURE 3. **Effect of miR-138 on role of SAL in HRMECs injury under hypoxic condition.** (**A**) MiR-138 abundance was measured using qRT-PCR in HRMECs after stimulation with hypoxia or SAL for 24 hours. (**B**) MiR-138 level was examined by qRT-PCR in miRNA NC or miR-138 mimic-transfected HRMECs. HRMECs were transfected with miRNA NC or miR-138 mimic before stimulation with hypoxia or SAL for 24 hours. Cell viability (**C**), proliferation (**D**), cycle process (**E**), apoptosis (**F**), protein levels of PCNA, cyclinD1, Bax, and Bcl-2 (**G**), secretion levels of TNF-α, IL-6, and IL-8 (**H**), and levels of MDA, ROS, and SOD (**I**) were measured using CCK-8, EdU staining, flow cytometry, Western blotting, and ELISA. $^{*}P < 0.05$.

suggested the establishment of hypoxic injury model of HRMECs.

SAL Attenuates Hypoxia-Induced HRMECs Injury

To explore the function of SAL on hypoxia-induced injury, HRMECs were incubated with SAL for 24 hours before hypoxia stimulation for 24 hours. SAL showed little effect on HRMECs viability, while it could rescue cell viability under hypoxic condition (Fig. 2A). The 20 µg/mL SAL with highest effect was chosen for subsequent experiments. EdU staining assay exhibited SAL treatment protected against hypoxia-induced proliferation inhibition in HRMECs (Fig. 2B). Furthermore, SAL mitigated hypoxia-induced cycle

A

WT-ROBO4-3'UTR:	5' ggcaacacaUCACUGCCACCAGCc 3'
miR-138 :	3' gccggacuaAGUG-UUGUGGUCGa 5'
MUT-ROBO4-3'UTR:	5' ggcaacacaUCACUGCGUGGUCGc 3'
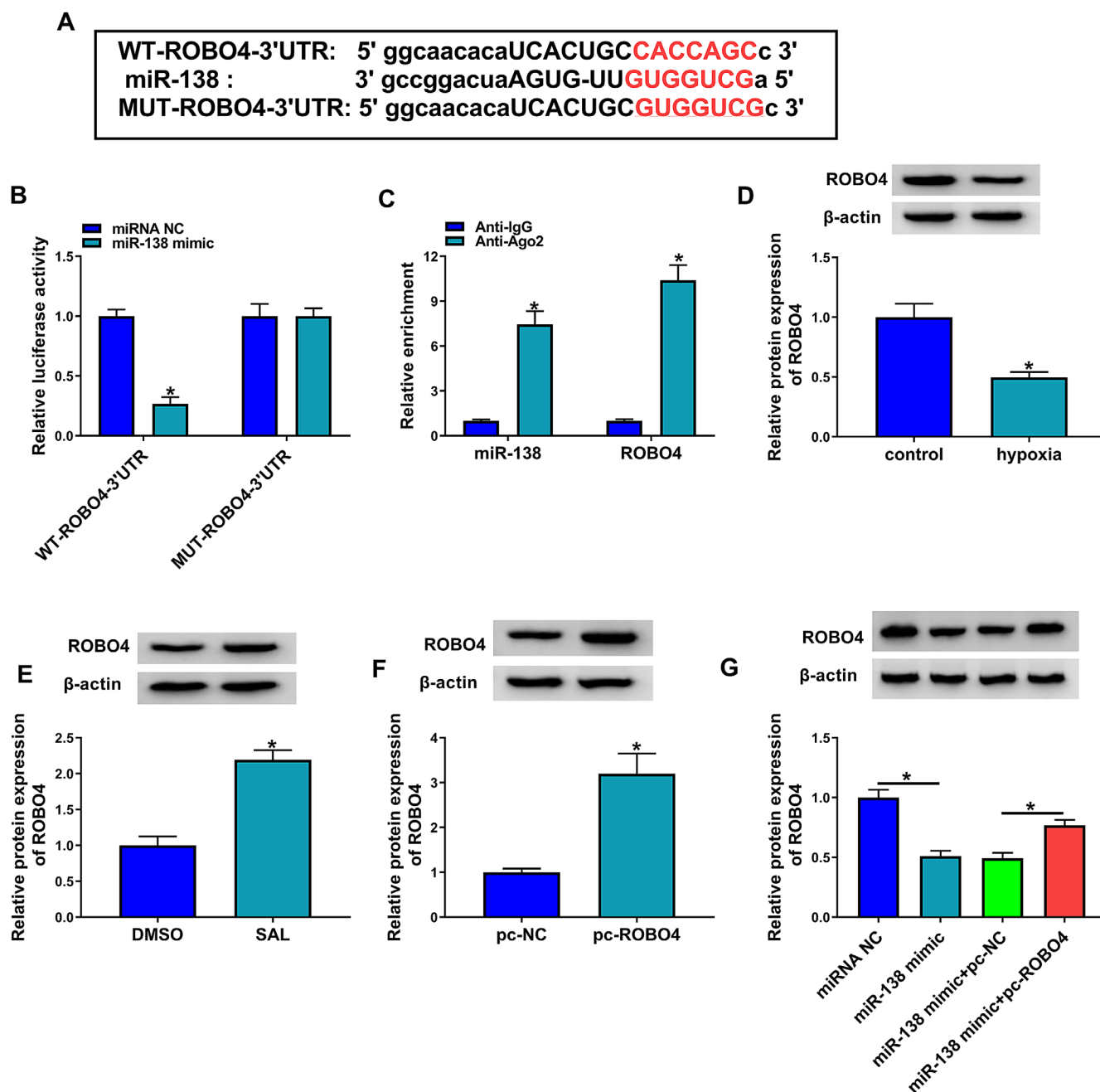
FIGURE 4. **Target of miR-138 on ROBO4.** (**A**) The target sites of miR-138 on ROBO4. (**B**) Luciferase activity was examined in HRMECs transfected with WT-ROBO4-3′UTR or MUT-ROBO4-3′UTR and miRNA NC or miR-138 mimic. (**C**) MiR-138 and ROBO4 levels were measured after RIP. (**D**) ROBO4 level was measured by Western blotting in HRMECs after stimulation with hypoxia. (**E**) ROBO4 expression was detected using Western blotting in HRMECs after stimulation with SAL for 24 hours under hypoxic condition. (**F**) ROBO4 expression was examined via Western blotting in pc-NC or pc-ROBO4-transfected HRMECs. (**G**) ROBO4 level was examined through Western blotting in HRMECs transfected with miRNA NC, miR-138 mimic, miR-138 mimic + pc-NC, or pc-ROBO4. $^{*}P < 0.05$.

arrest and apoptosis production (Figs. 2C, 2D). Additionally, SAL introduction reversed the regulation of hypoxia on levels of PCNA, cyclin D1, Bcl-2, and Bax (Fig. 2E). Moreover, SAL incubation attenuated hypoxia-mediated secretion of TNF-α, IL-6, and IL-8 (Fig. 2F). In addition, SAL exposure weakened hypoxia-induced oxidative stress by decreasing MDA and ROS levels and increasing SOD level (Fig. 2G). These results showed SAL prevented hypoxia-induced injury in HRMECs.

MiR-138 Upregulation Relieves the Effect of SAL in Hypoxia-Induced HRMECs Injury

To probe whether miR-138 was associated with the function of SAL, its expression change was detected in HRMECs after stimulation with SAL and hypoxia for 24 hours. MiR-138 abundance was significantly increased by hypoxia treatment, whereas introduction of SAL weakened this effect (Fig. 3A). In order to explore the role of miR-138 in SAL-mediated
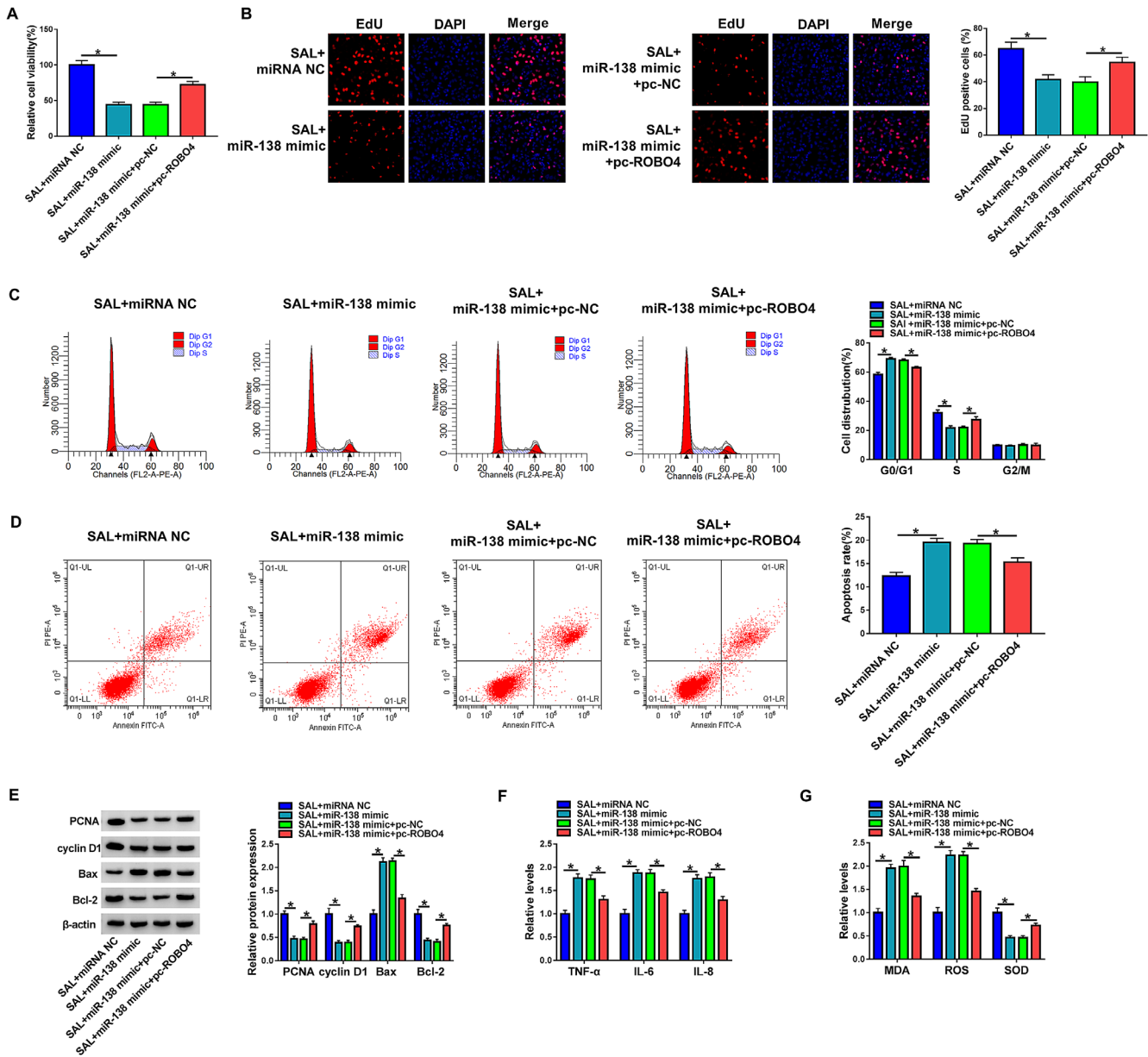
FIGURE 5. **Effect of miR-138/ROBO4 axis on role of SAL in HRMECs injury under hypoxic condition.** HRMECs were transfected with miRNA NC, miR-138 mimic, miR-138 mimic + pc-NC, or pc-ROBO4 before stimulation with hypoxia or SAL for 24 hours. Cell viability (**A**), proliferation (**B**), cycle process (**C**), apoptosis (**D**), expression of PCNA, cyclinD1, Bax, and Bcl-2 (**E**), secretion levels of TNF-α, IL-6, and IL-8 (**F**), and levels of MDA, ROS, and SOD (**G**) were detected with CCK-8, EdU staining, flow cytometry, Western blotting, and ELISA. $^{*}P < 0.05$.

regulation on hypoxia-induced injury, HRMECs were transfected with miRNA NC or miR-138 mimic before stimulation with SAL and hypoxia for 24 hours. The transfection of miR-138 mimic obviously elevated miR-138 abundance in HRMECs (Fig. 3B). Furthermore, miR-138 mimic weakened SAL-mediated promotion of cell viability and proliferation (Figs. 3C, 3D). In addition, miR-138 overexpression reversed SAL-mediated suppression of cycle arrest and apoptosis in hypoxia-treated HRMECs (Figs. 3E, 3F). Moreover, miR-138 upregulation partly abolished the regulatory effect of SAL on expression of PCNA, cyclin D1, Bcl-2 and Bax (Fig. 3G). Additionally, miR-138 addition weakened SAL-modulated inhibition of TNF-α, IL-6, and IL-8 levels under hypoxic condition (Fig. 3H). Besides, miR-138 upregulation reversed

SAL-mediated reduction of MDA and ROS, and elevation of SOD in hypoxia-stimulated HRMECs (Fig. 3I). These results indicated SAL mitigated hypoxia-induced injury in HRMECs by decreasing miR-138.

MiR-138 Targets ROBO4 in HRMECs

To analyze the downstream network of miR-138, the targets were predicted by starBase, which showed ROBO4 as a candidate. Predicted target sites of miR-138 on ROBO4 were shown in Figure 4A. In order to validate this prediction, we constructed the WT-ROBO4-3′UTR and MUT-ROBO4 3′UTR luciferase reporter vectors. MiR-138 mimic obviously declined the luciferase activity of WT-ROBO4-3′UTR,
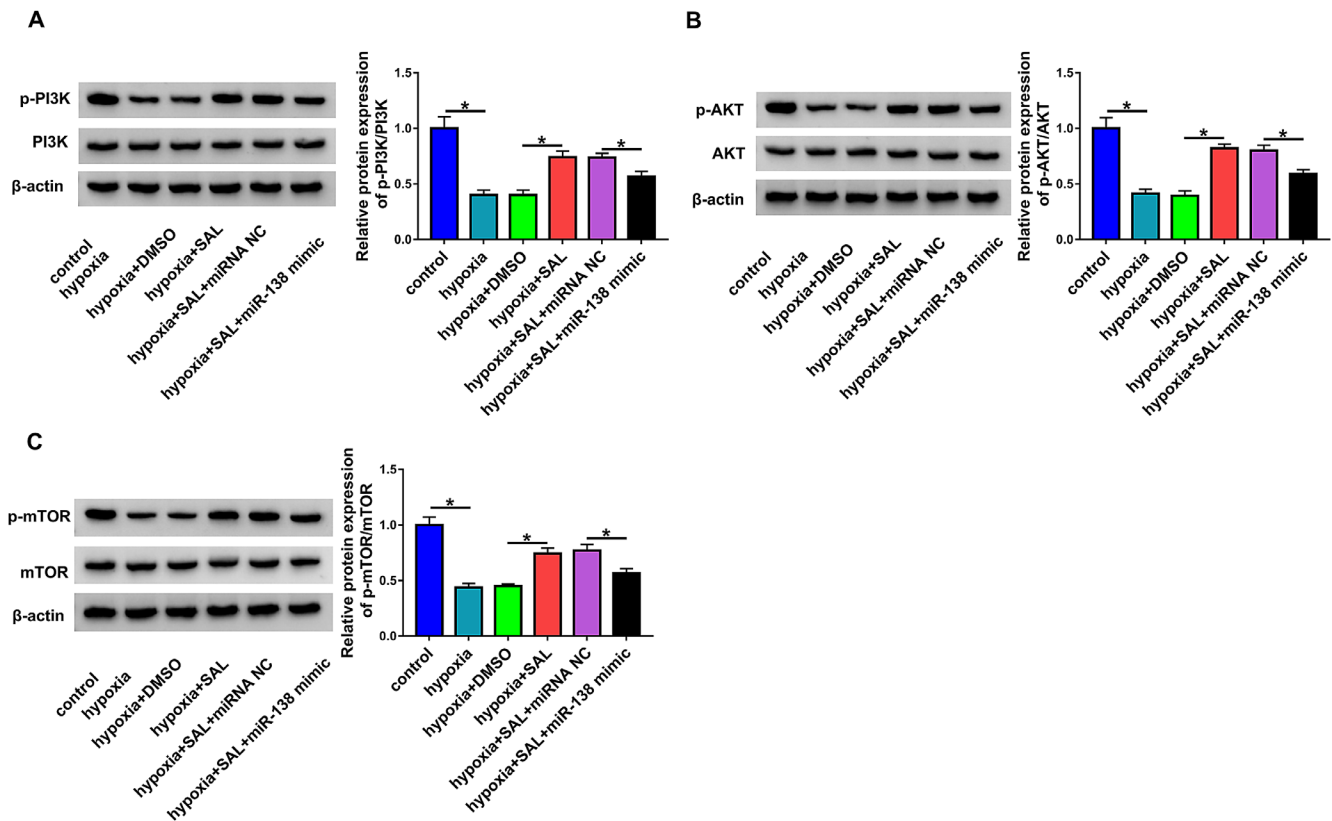
Figure 6. Influence of miR-138 on the PI3K/AKT/mTOR pathway. HRMECs were transfected with miRNA NC or miR-138 mimic before stimulation with hypoxia or SAL for 24 hours. PI3K and p-PI3K levels (**A**), AKT and p-AKT levels (**B**), mTOR and p-mTOR levels (**C**) were detected using Western blotting. $^{*}P < 0.05$.

although this effect was lost in MUT-ROBO4 3′UTR group (Fig. 4B). Furthermore, RIP assay displayed miR-138 and ROBO4 could be enriched in same complex (Fig. 4C). Additionally, ROBO4 protein level was markedly reduced in HRMECs after hypoxia stimulation (Fig. 4D). Moreover, in the hypoxia-stimulated cells, ROBO4 protein expression was obviously enhanced by SAL treatment (Fig. 4E). In addition, the effect of miR-138 on ROBO4 level was evaluated in HRMECs. ROBO4 abundance was evidently elevate by addition of pc-ROBO4 (Fig. 4F). Besides, ROBO4 protein expression was evidently decreased via miR-138 mimic, which was rescued by pc-ROBO4 (Fig. 4G). These data suggested miR-138 could target ROBO4 in HRMECs.

ROBO4 Reverses the Role of miR-138 in SAL-mediated Regulation on Hypoxia-Induced HRMECs Injury

To study whether ROBO4 was required for miR-138 to take part in SAL-mediated regulation on hypoxia-induced injury, HRMECs were transfected with miRNA NC, miR-138 mimic, miR-138 mimic + pc-NC, or pc-ROBO4 before stimulation with SAL and hypoxia for 24 hours. ROBO4 overexpression attenuated miR-138-mediated suppression of cell viability and proliferation in HRMECs treated with SAL under hypoxic condition (Figs. 5A, 5B). Furthermore, addition of pc-ROBO4 weakened miR-138-mediated promotion of cycle arrest and apoptosis in SAL-treated HRMECs under hypoxic condition (Figs. 5C, 5D). Additionally, ROBO4 restoration

reversed miR-138-mediated reduction of PCNA, cyclin D1, and Bcl-2, and increase of Bax in SAL-treated HRMECs under hypoxic condition (Fig. 5E). Moreover, ROBO4 upregulation mitigated miR-138-mediated promotion of TNF-α, IL-6 and IL-8 secretion (Fig. 5F). In addition, ROBO4 overexpression relieved miR-138-mediated increase of MDA and ROS levels, and decrease of SOD level (Fig. 5G). These data showed miR-138 regulated hypoxia-induced injury in HRMECs through ROBO4.

SAL Attenuates Hypoxia-Induced Inactivation of the PI3K/AKT/mTOR Pathway by Regulating miR-138

To explore whether the PI3K/AKT/mTOR pathway was involved in the function of SAL, related protein levels were examined in HRMECs transfected with miRNA NC or miR-138 mimic before treatment with hypoxia and SAL for 24 hours. As shown in Figure 6A to C, the phosphorylation levels of PI3K, AKT, and mTOR were obviously reduced by hypoxia treatment, and SAL incubation attenuated this effect. Moreover, the influence of SAL on the two signaling was reversed by miR-138 mimic (Figs. 6A–C). These results indicated SAL promoted the activation of the PI3K/AKT/mTOR pathway via decreasing miR-138 in hypoxia-treated HRMECs. Collectively, SAL prevented hypoxia-induced HRMECs injury through activating the PI3K/AKT/mTOR pathway through a miR-138/ROBO4 axis (Fig. 7).
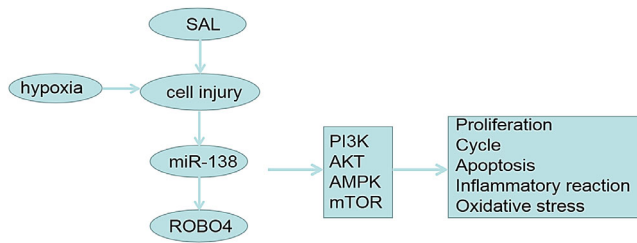
FIGURE 7. The schematic diagram of this study. SAL attenuated hypoxia-induced HRMECs injury by regulating miR-138/ROBO4 axis.

DISCUSSION

The hypoxia-induced retinal microvascular endothelial cell damage is associated with retinal damage in ischemic retinopathies.[1,3,4] In this research, we established the ischemic retinopathies model using hypoxia-stimulated HRMECs, and found hypoxia induced cell injury by decreasing cell proliferation, and promoting cycle arrest, apoptosis, inflammatory reaction, and oxidative stress, which was consistent with previous reports.[3,4] Moreover, we confirmed SAL exerted the protective function on hypoxia-induced injury through modulating the miR-138/ROBO4 axis.

Previous studies suggested SAL played a protective role in hypoxia-induced injury in neural stem cells, liver cells or cardiomyocytes.[9,10,21] Moreover, SAL had anti-inflammatory, anti-oxidative, and anti-apoptotic roles in endothelial cells.[22–24] In addition, SAL could attenuate retinal pigment epithelial cell damage under hydroperoxide or high glucose condition.[11,12] Hence, we hypothesized SAL might have a protective function on retinal microvascular endothelial cells under hypoxia condition. Consistent to this hypothesis, our study found SAL weakened hypoxia-induced HRMECs injury, indicating the potential therapeutic effect of SAL on ischemic retinopathies.

Next, we wanted to explore a potential mechanism. Former reports reported that SAL could have resulted in miRNA expression change, like miR-210, miR-138, and miR-21.[9,12,21] Here, we confirmed that SAL could decrease miR-138 expression in hypoxia-induced HRMECs, which was similar to that in high glucose-treated retinal pigment epithelial cells.[12] Wang et al. suggested that miR-138 promoted cardiac ischemia injury by inactivation of the SIRT1/PGC-1α pathway.[25] Moreover, Sen et al. reported miR-138 expression was enhanced in hypoxia-induced endothelial cells, and contributed to endothelial cell dysfunction.[15] These studies suggested miR-138 might contribute to hypoxia-induced injury. Similar to these reports,[12,15,25] we confirmed that miR-138 could increase hypoxia-induced HRMECs injury by abolishing the protective function of SAL, which also indicated SAL repressed hypoxia-induced HRMECs injury via decreasing miR-138.

The retinopathies are related to vascular permeability and neovascularization, and ROBO4 is an important protein involving in these processes.[16] Moreover, ROBO4 could attenuate inflammatory injury in endothelial cells by regulating TNF receptor-associated factor 7 (TRAF7).[26] Additionally, ROBO4 might have diverse roles in retinal microvascular endothelial cells under different stimulations like hyperglycemia or hypoxia.[18] In this study, we found ROBO4 expression was declined by hypoxia, which was consistent with a previous study.[18] Furthermore, we found ROBO4

expression was upregulated by SAL through miR-138. Functional analysis confirmed the protective role of ROBO4 in hypoxia-induced HRMECs injury, and indicated SAL could exert its activity through the miR-138/ROBO4 axis.

The AKT pathway is required for vascular growth, and it is inactivated under hypoxia in retinal endothelial cells.[27] Moreover, the activation of the PI3K/AKT signaling contributes to the survival of retinal microvascular endothelial cells.[28,29] Furthermore, SAL could attenuate hypoxia-induced neuronal injury by activating the PI3K/AKT/mTOR signaling.[9] In addition, SAL mitigated retinal pigment epithelial cell damage by increasing the activation of the PI3K/AKT pathway.[11,12] Similarly, our study found SAL might prevent hypoxia-induced HRMECs injury via activating the PI3K/AKT/mTOR pathway by miR-138, which was also in agreement with that in retinal pigment epithelial cell damage.[12]

In conclusion, SAL protected against hypoxia-induced HRMECs dysfunction, possibly by the miR-138/ROBO4 axis. This indicated a new insight in retinal microvascular endothelial cell damage, and provided a novel mechanism for understanding the pharmacological activity of SAL in ischemic retinopathies.

References

1. Kumar R, Mani AM, Singh NK, Rao GN. PKCtheta-JunB axis via upregulation of VEGFR3 expression mediates hypoxia-induced pathological retinal neovascularization. *Cell Death Dis*. 2020;11:325.

2. Uno K, Merges CA, Grebe R, Lutty GA, Prow TW. Hyperoxia inhibits several critical aspects of vascular development. *Dev Dyn*. 2007;236:981–990.

3. Yang B, Xu Y, Hu Y, et al. Madecassic Acid protects against hypoxia-induced oxidative stress in retinal microvascular endothelial cells via ROS-mediated endoplasmic reticulum stress. *Biomed Pharmacother*. 2016;84:845–852.

4. Hu Y, Yang B, Xu Y, Jiang L, Tsui CK, Liang X. FK506 suppresses hypoxia induced inflammation and protects tight junction function via the CaNNFATc1 signaling pathway in retinal microvascular epithelial cells. *Mol Med Rep*. 2017;16:6974–6980.

5. Magani SKJ, Mupparthi SD, Gollapalli BP, et al. Salidroside - Can it be a Multifunctional Drug? *Curr Drug Metab*. 2020;21:512–524.

6. Pu WL, Zhang MY, Bai RY, et al. Anti-inflammatory effects of Rhodiola rosea L.: A review. *Biomed Pharmacother*. 2020;121:109552.

7. Tang C, Zhao CC, Yi H, et al. Traditional Tibetan medicine in cancer therapy by targeting apoptosis pathways. *Front Pharmacol*. 2020;11:976.

8. Sun S, Tuo Q, Li D, et al. Antioxidant Effects of Salidroside in the Cardiovascular System. *Evid Based Complement Alternat Med*. 2020;2020:9568647.

9. Yan R, Xu H, Fu X. Salidroside protects hypoxia-induced injury by up-regulation of miR-210 in rat neural stem cells. *Biomed Pharmacother*. 2018;103:1490–1497.

10. Xiong Y, Wang Y, Xiong Y, Gao W, Teng L. Salidroside alleviated hypoxia-induced liver injury by inhibiting endoplasmic reticulum stress-mediated apoptosis via IRE1alpha/JNK pathway. *Biochem Biophys Res Commun*. 2020;529:335–340.

11. Yin Y, Liu D, Tian D. Salidroside prevents hydroperoxide-induced oxidative stress and apoptosis in retinal pigment epithelium cells. *Exp Ther Med*. 2018;16:2363–2368.

12. Qian C, Liang S, Wan G, Dong Y, Lu T, Yan P. Salidroside alleviates high-glucose-induced injury in retinal pigment epithelial cell line ARPE-19 by down-regulation of miR-138. *RNA Biol*. 2019;16:1461–1470.

13. Agrawal S, Chaqour B. MicroRNA signature and function in retinal neovascularization. *World J Biol Chem*. 2014;5:1–11.

14. Walz JM, Wecker T, Zhang PP, et al. Impact of angiogenic activation and inhibition on miRNA profiles of human retinal endothelial cells. *Exp Eye Res*. 2019;181:98–104.

15. Sen A, Ren S, Lerchenmuller C, et al. MicroRNA-138 regulates hypoxia-induced endothelial cell dysfunction by targeting S100A1. *PLoS One*. 2013;8:e78684.

16. Zhang F, Prahst C, Mathivet T, et al. The Robo4 cytoplasmic domain is dispensable for vascular permeability and neovascularization. *Nat Commun*. 2016;7:13517.

17. Xie J, Gong Q, Liu X, et al. Transcription factor SP1 mediates hyperglycemia-induced upregulation of roundabout4 in retinal microvascular endothelial cells. *Gene*. 2017;616:31–40.

18. Xie J, Liu X, Li Y, Liu Y, Su G. Validation of RT-qPCR reference genes and determination of Robo4 expression levels in human retinal endothelial cells under hypoxia and/or hyperglycemia. *Gene*. 2016;585:135–142.

19. Livak KJ, Schmittgen TD. Analysis of relative gene expression data using real-time quantitative PCR and the 2(-Delta Delta C(T)) Method. *Methods*. 2001;25:402–408.

20. Li JH, Liu S, Zhou H, Qu LH, Yang JH. starBase v2.0: decoding miRNA-ceRNA, miRNA-ncRNA and protein-RNA interaction networks from large-scale CLIP-Seq data. *Nucleic Acids Res*. 2014;42:D92–D97.

21. Liu B, Wei H, Lan M, Jia N, Liu J, Zhang M. MicroRNA-21 mediates the protective effects of salidroside against hypoxia/reoxygenation-induced myocardial oxidative stress and inflammatory response. *Exp Ther Med*. 2020;19:1655–1664.

22. Wang Y, Su Y, Lai W, et al. Salidroside restores an anti-inflammatory endothelial phenotype by selectively inhibiting endothelial complement after oxidative stress. *Inflammation*. 2020;43:310–325.

23. Hu R, Wang MQ, Ni SH, et al. Salidroside ameliorates endothelial inflammation and oxidative stress by regulating the AMPK/NF-kappaB/NLRP3 signaling pathway in AGEs-induced HUVECs. *Eur J Pharmacol*. 2020;867:172797.

24. Zhao D, Sun X, Lv S, et al. Salidroside attenuates oxidized low density lipoprotein induced endothelial cell injury via promotion of the AMPK/SIRT1 pathway. *Int J Mol Med*. 2019;43:2279–2290.

25. Wang C, Sun X, Qiu Z, Chen A. MiR-138-5p exacerbates hypoxia/reperfusion-induced heart injury through the inactivation of SIRT1-PGC-1alpha. *Inflamm Res*. 2019;68:867–876.

26. Shirakura K, Ishiba R, Kashio T, et al. The Robo4-TRAF7 complex suppresses endothelial hyperpermeability in inflammation. *J Cell Sci*. 2019;132.

27. Sun JF, Phung T, Shiojima I, et al. Microvascular patterning is controlled by fine-tuning the Akt signal. *Proc Natl Acad Sci USA*. 2005;102:128–133.

28. Ohashi H, Takagi H, Oh H, et al. Phosphatidylinositol 3-kinase/Akt regulates angiotensin II-induced inhibition of apoptosis in microvascular endothelial cells by governing survivin expression and suppression of caspase-3 activity. *Circ Res*. 2004;94:785–793.

29. Lu JM, Zhang ZZ, Ma X, Fang SF, Qin XH. Repression of microRNA-21 inhibits retinal vascular endothelial cell growth and angiogenesis via PTEN dependent-PI3K/Akt/VEGF signaling pathway in diabetic retinopathy. *Exp Eye Res*. 2020;190:107886.